DOI 10.15622/ia.25.4.11

A. VYBORNOV, A. TROFIMOV, S. PASHHENKO, A. KRYLOV, A. SHISHKIN, O. DE-MONDERIK

ENHANCEMENT OF RF FIELD STABILITY IN AN LLRF SYSTEM VIA INCLUSION OF A SECOND-ORDER INTEGRAL TERM IN THE PID CONTROLLER TRANSFER FUNCTION

Vybornov A., Trofimov A., Pashhenko S., Krylov A., Shishkin A., De-Monderik O. **Enhancement of RF Field Stability in an LLRF System via Inclusion of a Second-Order Integral Term in the PID Controller Transfer Function.**

Abstract. The paper addresses the problem of improving the amplitude and phase stabilization accuracy of the high-frequency field in low-level radio frequency (LLRF) control systems for charged particle accelerators. It is shown that low-frequency disturbances caused by power supply ripple, thermal drifts, and load variations are the dominant sources of stability degradation. It is demonstrated that the classical PID controller structure is fundamentally limited in suppressing such disturbances due to the trade-off between low-frequency gain and stability margins. A modified controller structure with a second-order integral component is proposed. The proposed approach increases the system astatism order and provides -40 dB/decade slope of the amplitude response in the low-frequency region, resulting in significantly enhanced suppression of quasi-static and slowly varying disturbances. A mathematical model of the control system is developed to capture the essential dynamic behavior of the RF chain. In addition, a nonlinear control strategy is introduced based on delayed activation of the second-order integral component, which prevents an increase in the transient duration while preserving disturbance rejection performance. Simulation and experimental results demonstrate that the proposed controller achieves more than 20 dB improvement in dynamic range and amplitude stability compared to typical modern systems, along with at least a tenfold reduction in phase root-mean-square deviation. These results confirm that introducing a second-order integral component into the controller structure is an effective method for enhancing RF signal stabilization accuracy while maintaining system stability and robustness.

Keywords: RF signal stabilization, LLRF system, RF path, FPGA, low-frequency disturbance suppression, cyclotron RF system.

1. Introduction. Stabilization of high-frequency (RF) field parameters is a critical task for improving the performance of many modern systems in which it is applied. In accelerator technology intended for physical experiments, this task is performed by a Low-Level Radio Frequency (LLRF) system, which generates the RF signal and stabilizes its amplitude and phase directly at the electrodes of the accelerating structure [1 – 8]. In cyclotrons, beam acceleration occurs between the *dee* (anode) and the *anti-dee* (cathode).

At present, the amplitude stability of such systems is approximately 80-86 dB (with a root-mean-square (RMS) deviation of about 0.01-0.005 dB), RMS deviation of the initial phase σ_φ ranges from 0.01 to 0.1 degrees due to the use of digital technologies based on field-programmable gate arrays

(FPGAs). This performance reduces the intensity losses of the accelerated ion beam by several times compared to systems without stabilization [9].

The requirements for the accelerated ion beam current are continuously increasing; consequently, the losses caused by insufficient RF field stability are also increasing. Therefore, it is necessary to synthesize a system with a higher-quality controller without a significant increase in control loop complexity.

Hereinafter, the term “RF field” is partially replaced by “RF signal” (or simply “signal”), which denotes the high-frequency electromagnetic field in the accelerating resonator represented in the form of a complex envelope suitable for digital signal processing. This substitution is introduced because the term “RF field” is not applicable to all components of the control system (e.g., the digital generator and other digital processing elements).

2. Description of the RF Loop. The control system shown in Figure 1 is somewhat simplified. It includes the following functional elements:

1. Reference signal generator (RF Actuator);
2. Vacuum tube power amplifier with its own resonant circuit (RF Amplifier);
3. Resonant circuit of the accelerating structure (Cavity);
4. RF signal transmission and processing path introducing a pure time delay (Delay);
5. Complex envelope detector (RF Detector) in the feedback path;
6. RF Controller.

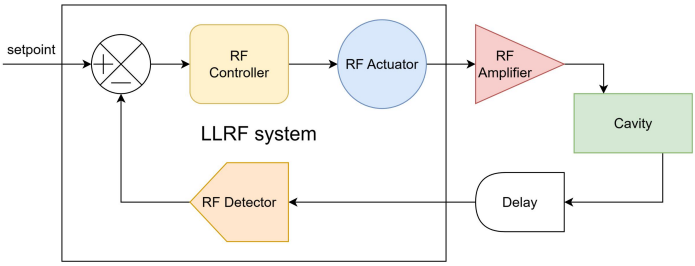

Fig. 1. Functional diagram of the main RF field stabilization loop of the ion accelerator

The entire LLRF system is clocked from a common reference clock generator. Thus, all sinusoidal signal generators and local oscillators are synchronized with each other. The RF actuator generates a sinusoidal signal $V(t)$ with a specified amplitude A, carrier angular frequency f_{cr} and initial phase φ :

$$V(t) = A\cos\left(2\pi \times f_{cr} t + \varphi\right), \quad (1)$$

where t is time.

The RF field is the plant whose parameters must be maintained with maximum stability directly at the electrodes of the resonant system by means of a closed-loop automatic control system. The feedback path includes a delay and an RF detector that extracts the complex envelope of the signal. Depending on the selected stabilization method, the complex envelope may be further converted into amplitude and phase [10, 11]. Subsequently, through negative feedback, the controller generates a control action aimed at minimizing the error.

3. Problem Analysis. Consider the RF field at the electrode of the accelerating structure of a cyclotron. The frequency stability is directly determined by the stability of the reference clock generator of the digital part of the system. The amplitude and initial phase of the signal may be subject to distortions and are therefore treated as time-dependent functions. Since the carrier frequency of the signal remains constant, it is appropriate to analyze disturbances in terms of the complex envelope of the signal, which is described as follows:

$$V_{IQ}(t) = A(t) \times \left[\cos\left(\varphi(t)\right) + j\sin\left(\varphi(t)\right)\right], \quad (2)$$

where the real part (in-phase component):

$$A(t) \times \cos\left(\varphi(t)\right) = I(t), \quad (3)$$

and the imaginary part (quadrature component):

$$A(t) \times \sin\left(\varphi(t)\right) = Q(t). \quad (4)$$

In this case, the carrier frequency of the signal is not relevant. Part of the system is implemented in the digital domain; therefore, it is assumed that the second harmonic of the carrier frequency is less than half of the system sampling frequency (i.e., no aliasing occurs).

Low-frequency fluctuations arise due to the following reasons:

1. Temperature drift of the R, L, and C parameters of the resonant circuit causes a drift of the resonant frequency. As a result, amplitude and initial phase drift occur;

2. Non-ideal power supply of the vacuum tube amplifier, which introduces disturbances at the angular mains frequency f_m (50, 60 Hz) and its harmonics (amplitude modulation);

3. Temperature drift of the parameters of the path from the digital to analog converter to the electrode, causing amplitude and phase distortions.

Analysis of the sources of instability shows that the dominant contribution to the degradation of amplitude and phase stability (or stability of the complex envelope) is due to disturbances at the mains frequency and its harmonics in the vacuum tube amplifier. Instability of the power supply of the power amplifier leads to periodic fluctuations of the anode (or collector) voltage $\Delta V_p(t)$, which can be represented as a harmonic series:

$$\Delta V_p(t) = \sum_{n=1}^{\infty} V_n \cos\left(n \times \omega_m t + \psi_n\right), \tag{5}$$

where n is the harmonic number (a positive integer), V_n is the amplitude of the n-th harmonic, and ψ_n is the initial phase of each n-th harmonic of the ripple (determined by phase shifts in the rectifier, filters, and load).

In real power supplies, the distribution of fluctuations is determined by the type of rectifier and filter. The most pronounced disturbances occur at the following harmonics:

- the fundamental mains harmonic;
- the second harmonic, which is most pronounced in full-wave rectification systems and typically dominates;
- the third harmonic, which arises due to load nonlinearity and circuit asymmetry.

In practical systems, the second harmonic of the mains is most often the dominant component determining the spurious-free dynamic range (SFDR) of the RF field, which can decrease to 20 dB. Such fluctuations are practically not suppressed by the resonator itself and, therefore, require effective compensation by means of the automatic control system.

4. Controller Synthesis Criteria. For the synthesis of an automatic control system, it is necessary to formulate criteria that define the performance requirements. In a number of studies, the main performance indicators are the maximization of the signal-to-noise ratio (SNR), which determines the quality of amplitude stabilization, and the minimization of the signal σ_φ. However, in practical control systems, robustness is also an important requirement.

Robustness ensures the preservation of stability and the required control performance over the entire permissible range of variations in the RF system parameters. With sufficient controller robustness, additional parameter optimization may not be required.

Thus, the main controller synthesis criteria are:

1. SNR above 100 dB and σ_φ less than 0.001 degrees;
2. Robustness;
3. Capability for rigorous analytical analysis of the control system.

The controller must ensure stability and acceptable control performance over the entire range of permissible variations of the plant parameters. Such variations include:

- variation of the quality factor of the amplifier resonator or the accelerating structure resonator when the load is removed from the output of the resonant circuit, where the load is the ion beam;
- variation of the power amplifier gain;
- variation of the delay in the path (e.g., due to changes in cable length after maintenance).

The number of controller synthesis criteria in real control systems is significantly greater than the set of formalized performance metrics used in design. In addition to energy characteristics, statistical measures of instability, stability margins, and robustness, constraints on response speed, parametric uncertainty, computational resources, and delays associated with digital implementation are also taken into account. The specific set of criteria is determined by the adopted plant model and the problem formulation.

Achieving the best values of the selected criteria does not constitute proof of global optimality of the controller, since it always depends on the employed model, constraints, the class of admissible structures, and the nature of disturbances. Therefore, the synthesized controller can be regarded as pseudo-optimal – optimal within the adopted model, selected criteria, and the considered class of control structures.

5. Controller Model Synthesis. To suppress drift and other disturbances in the system, a proportional-integral (PI) controller is most commonly used [12–20]. The PI controller belongs to the class of linear controllers and is widely used due to its high efficiency, the possibility of rigorous analytical analysis of stability and dynamic properties, as well as the relative simplicity of hardware and software implementation. Its transfer function is given as follows:

$$C_{PID}(s) = K_p + \frac{K_i}{s} + K_d \times s\,, \tag{6}$$

where K_p is the proportional gain, K_i is the integral gain, K_d is the derivative gain, and s is the Laplace transform variable.

Typically, the settling time of such systems lies in the range of 20 to 100 microseconds, which is significantly shorter than the period of a single mains harmonic. However, even in the case of superconducting resonators [1, 8], where the settling time can reach 25 milliseconds, suppression of mains harmonics remains insignificant. Thus, the disturbance occurs at sufficiently low frequencies; therefore, the contribution of the derivative term is negligible, although it may be used to increase the stability margin of the system.

Increasing the integral gain K_i leads to a shift of the open-loop magnitude response in the low-frequency region without changing its slope. However, in the presence of pure delay and inertial elements of the plant, an increase in low-frequency gain is inevitably accompanied by a reduction in phase margin. In the limiting case, this results in oscillatory behavior or loss of stability. Therefore, the classical **PID** controller structure has a fundamental limitation: it allows an increase in the suppression of low-frequency disturbances only within the bounds permitted by stability requirements.

From the viewpoint of the sensitivity magnitude response, the slope of the integral term is -20 dB per decade, and the gain does not change this slope but shifts it by a value of $20\log_{10}(K_i)$. To improve the suppression of low-frequency disturbances, it is necessary to increase the steepness of the sensitivity function roll-off toward lower frequencies.

One possible solution is to introduce an additional second-order integral term. In this case, the controller model can be represented as follows:

$$C(s) = K_p + \frac{K_i}{s} + \frac{K_{i2}}{s^2} + K_d \times s\,. \tag{7}$$

In the low-frequency region, when the second-order integral term dominates, the slope of the magnitude response increases to -40 dB per decade. Accordingly, the sensitivity function of the closed-loop system $S(s)$ decreases faster as $\omega \to 0$, which ensures more effective suppression of quasi-static and slowly varying disturbances. Hereinafter, this controller is denoted as **PII²D**.

The block diagram of this controller becomes only slightly more complex compared to the classical PID from the standpoint of hardware

implementation, since it is sufficient to integrate the output of the first-order integral term, as shown in Figure 2.

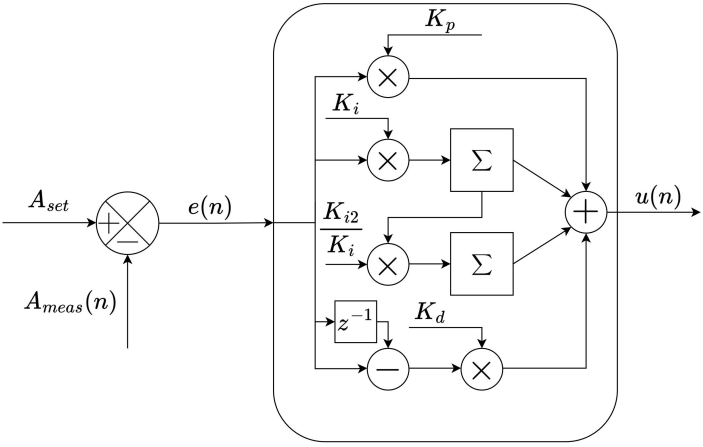

Fig. 2. Block diagram of an example digital implementation of the PII²D controller

If the multiplication by the gain K_i is performed before error accumulation, which is appropriate from the standpoint of FPGA resource utilization, then K_{i2} should be scaled inversely proportional to K_i. In digital implementation, it is necessary to account for nonlinear constraints associated with saturation of the control signal and the integral terms in order to prevent numerical overflow. These constraints affect the transient response of the system, in particular the settling time and overshoot.

Thus, the synthesis of the controller model reduces to the formation of a structure that theoretically ensures:

- an increase in the system type;
- enhanced suppression of low-frequency disturbances;
- preservation of a positive phase margin;
- limited parametric dimensionality;
- the possibility of analytical determination of initial ranges of the coefficients.

In LLRF systems, the choice of a control algorithm is not limited to the selection of a particular controller. Depending on the accelerator type, the RF chain architecture, the operating mode of the resonator, and the required field stability performance, different RF field control strategies may be employed. In particular, feedback and feedforward control loops [2, 21],

control in amplitude-phase coordinates and in Cartesian I/Q coordinates, generator-driven operation, self-excited loops, phase-locked loops, as well as analog and digital implementations, single-cavity control, and vector-sum control are commonly discussed in the literature. This indicates that a particular controller represents only one element of the overall LLRF system architecture and is not the sole factor determining its functional capabilities.

The approach proposed in this work, based on the use of a controller with a second-order integral component, does not restrict the applicability of the control strategies mentioned above. It is not intended to be opposed to auxiliary methods that complement the stabilization loop, such as feedforward compensation, adaptive feedforward, frequency-selective filtering, or different coordinate representations of the controlled variables. On the contrary, the considered algorithm can be integrated into an existing LLRF control architecture as a modification of the main feedback path, aimed at increasing the system type and improving the rejection of low-frequency and quasi-static disturbances.

Among the auxiliary methods, adaptive feedforward is the most relevant approach for comparison with the proposed controller, since it is also aimed at improving disturbance compensation in RF field control systems. In LLRF applications, adaptive feedforward is typically used to compensate repetitive and reproducible disturbances by updating a feedforward table for subsequent pulses, cycles, or operating conditions on the basis of the error between the setpoint and the measured RF field. This approach can be effective for compensating deterministic effects such as beam loading, slow variations in system parameters, and operating-point drift. However, its performance depends on the learning procedure, the accuracy of the feedforward table update, and the repeatability of the disturbance structure.

At the same time, adaptive feedforward is generally not used as a replacement for the feedback loop, but rather as an additional compensation channel. For deviations that arise directly during operation and do not necessarily have a known or reproducible structure in advance, the feedback loop remains the primary control mechanism. Therefore, in this work, the proposed PII²D controller is compared with a conventional PID controller, which is used as the baseline due to its widespread practical use, structural simplicity, well-established tuning procedures, and direct belonging to the same class of feedback controllers. This comparison makes it possible to evaluate specifically the contribution of the additional second-order integral component to the rejection of low-frequency disturbances, without mixing this effect with the specific features of auxiliary feedforward or adaptive compensation channels.

6. Mathematical Model of the Control System. Consider an idealized model of the RF system of the accelerator. To simplify the analysis, all nonlinear transfer functions (including those in the z-domain) are approximated in the continuous Laplace domain.

If stabilization of the complex envelope is considered such that the difference between the measured and set phase is equal to zero, then the controllers operating in the I and Q channels can be chosen with identical coefficients. In this case, the complex-envelope stabilization system can be reduced to an equivalent problem of RF signal amplitude stabilization for small variance of phase fluctuations. The resulting model remains applicable to the complex envelope, which corresponds to an implementation with two controllers operating in parallel for the in-phase and quadrature components.

The system consists of the following cascaded elements with their corresponding transfer functions:

1. RF actuator. It generates the reference RF signal and performs quadrature modulation based on the input in-phase and quadrature components. In the idealized model, the dynamic properties of this block are neglected, and it is described by a constant gain:

$$G_{gen}(s) = K_{gen}. \tag{8}$$

2. RF amplifier. The power amplifier increases the signal level to the value required to excite the resonant circuit. Within the idealized model, the amplifier is assumed to be linear and is described by the following transfer function in the complex-envelope domain of the input signal:

$$G_{amp}(s) = \frac{K_{amp}}{(1 + s\mathrm{T}_{amp})}, \tag{9}$$

where T_{amp} is the time constant of the amplifier transient response, and K_{amp} is the gain.

3. Cavity. In the complex-envelope domain, the resonant circuit is described as a first-order inertial element with the resonator time constant T_{cav}:

$$G_{cav}(s) = \frac{K_{cav}}{1 + s\mathrm{T}_{cav}}, \tag{10}$$

where K_{cav} is the resonator gain. During accelerator operation, T_{cav} may vary significantly. This depends on the load in the resonant circuit, which is the beam of charged particles. As a rule, the ratio of the unloaded quality factor to the loaded quality factor is equal to 2. Thus, the transient time constant also changes by a factor of 2. The system must remain stable in both cases; however, under load, the settling time of the closed-loop system should be minimized, in which case the system can be considered robust.

4. Delay. Cable lines, the transmission path, as well as signal processing in the LLRF hardware introduce a pure time delay of duration τ_d. In the continuous Laplace domain, such a delay is described by the transfer function:

$$P(s) = e^{-s\tau d}. \tag{11}$$

5. RF detector. Detects the complex envelope of the signal. It is a linear element, since complex-envelope detection is performed using a local oscillator (LO) and, by means of a cascade of two moving-average filters $H_{MA}(z)$, suppresses the linear distortion at frequency $2\omega_{cr}$ that arises after multiplication of the RF feedback signal and the LO signal. In addition, the detector has a gain that scales the feedback signal such that the product of all gains in the loop is equal to 1. The approximation of the moving-average transfer function and the transfer function of the detector are given by:

$$H_{MA}(s) = \frac{1 - e^{-sT_{MA}}}{sT_{MA}}, \tag{12}$$

$$H(s) = K_a H^2{}_{MA}(s). \tag{13}$$

6. Controller. A PID controller with an additional second-order integral term. Its transfer function (7) was considered earlier.

Thus, the open-loop transfer function is written as follows:

$$L(s) = G_{gen}(s) \times G_{amp}(s) \times G_{cav}(s) \times C(s) \times H(s), \tag{14}$$

$$L(s) = \frac{\left(K_p + \frac{K_i}{s} + \frac{K_{i2}}{s^2} + K_d \times s\right) e^{-\tau_d s} \times \left(1 - e^{-2T_{MA}s}\right)}{(1 + s\mathrm{T}_{amp})(1 + s\mathrm{T}_{cav}) \times sT_{MA}^2}. \quad (15)$$

The exponential function is not a rational function. To enable the application of standard methods of analysis and synthesis of control systems, the exponential delay function is approximated by a rational function. The most common approach is the Pade approximation. In the general case, the Pade approximation of order (*n, n*) is given by:

$$e^{-s\tau_d} \approx \frac{\sum_{k=0}^{n} a_k (s\tau_d)^k}{\sum_{k=0}^{n} b_k (s\tau_d)^k}, \quad (16)$$

where the coefficients of the numerator and denominator are determined by:

$$a_k = (-1)^k \frac{(2n-k)!n!}{(2n)!k!(n-k)!}$$
$$b_k = \frac{(2n-k)!n!}{(2n)!k!(n-k)!}, \quad k = 0,1,...,n. \quad (17)$$

The order of the polynomial was selected empirically and set to 63.

Thus, the block diagram of the simplified (but sufficient for qualitative analysis) RF voltage stabilization system is as follows, as shown in Figure 3.

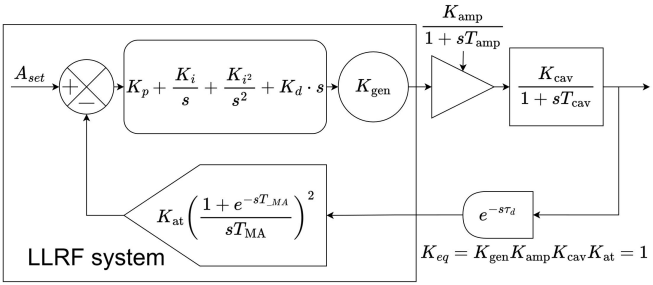

Fig. 3. Block diagram of the approximated RF field stabilization system with respect to the envelope

7. Dynamic Analysis of the Control System. Let the system parameters be set to the following values, for which stability is guaranteed:

1. $T_{amp} = 3 \times 10^{-7}$;
2. $T_{cav} \approx 3.687 \times 10^{-5}$ sec. for the loaded resonator and $2 \times T_{cav}$ for the unloaded resonator;
3. $\tau_d = 1,$ us ;
4. $T_{MA} = 2048,$ ns
5. $K_p = 14$;
6. $K_i = 0.008 / dt$;
7. $K_{i^2} = 0.0000004 / (dt)^2$;
8. $K_d = 6000 \times dt$, where dt is the sampling period of the digital system equal to 4 ns (specified for simplification of implementation in real hardware).

The most important indicators of dynamic analysis for evaluating the stabilization quality of such systems are the sensitivity function [10] and the transient response (the system response to a unit step input). The sensitivity function is defined as:

$$S(s) = \frac{1}{1 + L(s)}, \tag{18}$$

The function $|S(s)|$ characterizes the suppression of external disturbances acting on the plant. Thus, $S(s)$ can be used to assess the optimality of the controller, as it reflects the degree of suppression of harmonic distortions corresponding to disturbances at the mains frequency and its harmonics. Based on system analysis, it is assumed that the amplitude of such distortions can reach -20 dB. Therefore, to achieve amplitude stability exceeding 100 dB, it is sufficient to suppress distortions at the third harmonic of the mains by more than 85 dB.

In addition, it is important to evaluate the peak sensitivity:

$$M_S(s) = \max |S(s)|, \tag{19}$$

as well as the peak complementary sensitivity:

$$M_T(s) = \max\left|T(s)\right|, \tag{20}$$

where the closed-loop transfer function is defined as:

$$T(s) = \frac{L(s)}{1+L(s)}. \tag{21}$$

For clarity, the dynamic analysis is performed for both the classical PID controller and the synthesized controller. As discussed earlier, the transfer function of the system varies during accelerator operation due to changes in load. In this case, the system should exhibit the highest stabilization efficiency and the shortest transient duration under maximum load conditions. This is because, with increasing beam input intensity, the losses of accelerated ions increase. In the absence of load, it is sufficient for the system to remain stable. The sensitivity magnitude response under loaded conditions is shown in Figure 4.

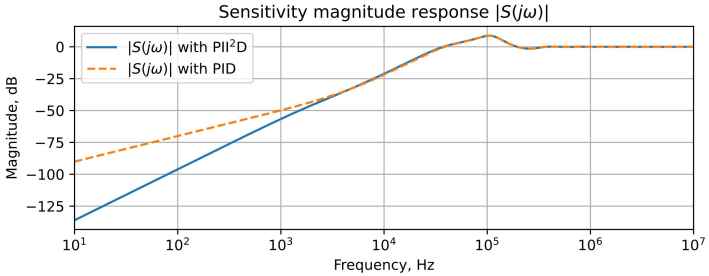

Fig. 4. Sensitivity magnitude response of the control system with classical PID and PII²D controllers (loaded condition)

As expected, the slope in the low-frequency region is 40 dB per decade for the synthesized controller. At higher frequencies, the first-order integral term dominates; therefore, the responses are nearly identical above 10 kHz. Preservation of the first-order integral term ensures system stability.

Table 1 presents data on phase margin, gain margin, sensitivity peak, complementary sensitivity peak and the level of suppression of modulations at 150 Hz for the classical PID and PII²D controllers.

The sensitivity peak and complementary sensitivity peak of the proposed controller are slightly reduced, which is a favorable result. It should be noted that, according to the Bode sensitivity integral, a reduction

in sensitivity in the low-frequency region is inevitably accompanied by its redistribution toward higher frequencies.

In the considered system, the peak value of the sensitivity function is slightly lower than that of the classical PID controller. It can be expected that further increase in the gain of the second-order integral term would lead to an additional reduction of the sensitivity peak. At the same time, the sensitivity integral is preserved due to an increase in the high-frequency region (in this case, starting from approximately 10 kHz), which reflects the fundamental trade-off between disturbance rejection and robustness.

The phase margin slightly increases in the case of the loaded resonator and decreases by less than 1.5 degrees under no-load conditions. At the same time, attenuation of mains harmonics increases by more than 22 dB.

The derivative term allows an increase in phase margin within the range of possible variations of the system transfer function and thus improves robustness. If it is excluded, a reduction of the remaining controller gains may be required, which would affect the attenuation of mains harmonics. In general, the derivative gain does not require continuous tuning. According to data obtained during long-term operation and tuning of cyclotrons at the Flerov Laboratory of Nuclear Reactions, it is sufficient to determine the value of K_d at which the system approaches instability and divide it by 2. This provides a coarse but effective result and does not require additional experiments, thereby accelerating the deployment of the LLRF system.

Table 1. Results of the system dynamic analysis

Parameter	PID	PII²D
Phase margin (T_{cav}), °	37,21	37,67
Phase margin ($2 \times T_{cav}$), °	35,10	33,76
Gain margin (T_{cav}), dB	4,21	4,24
Gain margin ($2 \times T_{cav}$), dB	10,16	10,19
Sensitivity peak, dB	8.76	8.71
Complementary sensitivity peak, dB	5.29	5.21
Attenuation at 150 Hz, dB	66,53	89,00

Next, consider the transient response with saturation control (from 0 to 4), as shown in Figure 5.

As can be seen, the settling time of the system with the PII²D controller increases. To apply such a controller in linear accelerator systems, where such transient processes are a regular occurrence, it is necessary to introduce activation of the second-order integral term after the transient process. This can be implemented such that, after the start of the

transient, at a time T_{sys} equal to the settling time of the system with the classical PID controller, accumulation in two error integrators – independent of the first integrator of the first-order integral term – is activated. That is, its implementation differs from the controller shown in Figure 2. Let the start of the transient process be defined as:

$$t_0 = 0\,. \tag{22}$$

Then, the transfer function of such a controller is given by:

$$C_{non-lin}(s) = \begin{cases} K_p + \dfrac{K_i}{s} + K_d \times s, & t < T_{sys} \\ K_p + \dfrac{K_i}{s} + \dfrac{K_{i2}}{s^2} + K_d \times s, & t \geq T_{sys} \end{cases}. \tag{23}$$

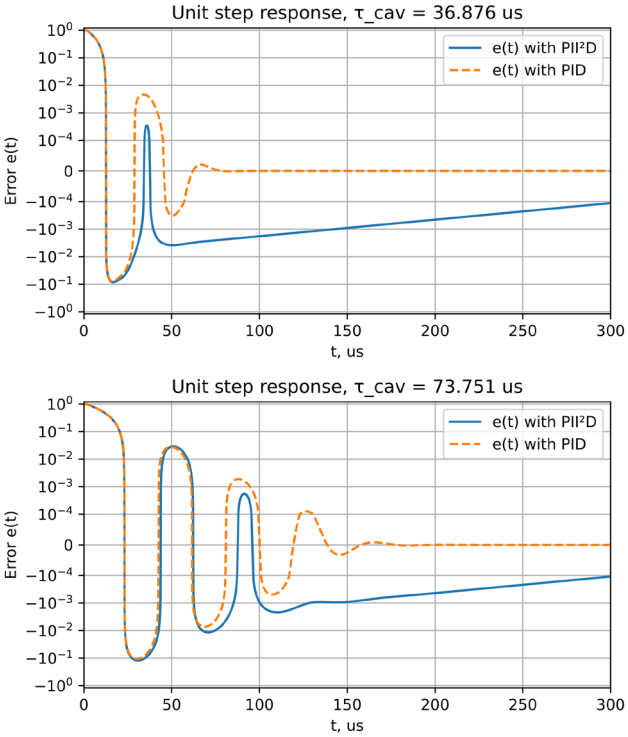

Fig. 5. Unit step response of the system (linear scale from -10^{-4} to 10^{-4})

Assume that for the considered system T_{sys} is equal to 100 microseconds. Then, the response of the system with controller (23) is as shown in Figure 6.

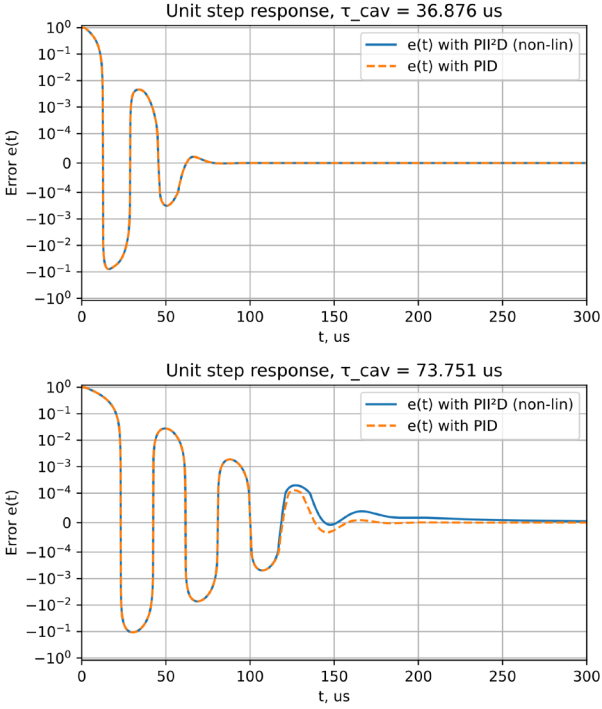

Fig. 6. Unit step response of the system with a nonlinear controller (linear scale from -10^{-4} to 10^{-4})

The difference in settling time becomes negligible. The results indicate that the use of such a controller is feasible in all types of accelerator systems.

8. Hardware Implementation and Experiment. The hardware implementation consists of synthesizing the “IQ_Controller” module in the “SystemVerilog” hardware description language, followed by implementation on an FPGA. A detailed hardware description does not provide scientific value; therefore, only key parameters are presented:

1. FPGA sampling frequency: 250 MHz;
2. DAC sampling frequency: 500 MHz;
3. DAC resolution: 16 bits;

4. ADC resolution: 14 bits;
5. Analog-to-digital converter (ADC) sampling frequency: 250 MHz;
6. Carrier frequency of the reference signal f_{cr} = 8.632 MHz.

An example implementation of the controller is available in the repository at [22].

In this case, either the in-phase or quadrature component is applied at the input. To stabilize the entire signal, the controllers must be connected in parallel.

The transfer functions of the resonators are replaced by digital IIR (infinite impulse response) low-pass filters with equivalent time constants tau placed before the RF actuator. The pure delay is implemented using a FIFO (first-in, first-out) buffer. Amplitude modulation is implemented on the FPGA after the RF actuator. The evaluation is performed based on acquired complex-envelope data consisting of 16,384 samples with a sampling rate of 20,480 Hz. As a result of the experiment, the magnitude response of the complex envelope, the spurious-free dynamic range (SFDR), and σ_φ are obtained: for the **PID** controller in Figure 7 and for the **PII²D** controller in Figure 8.

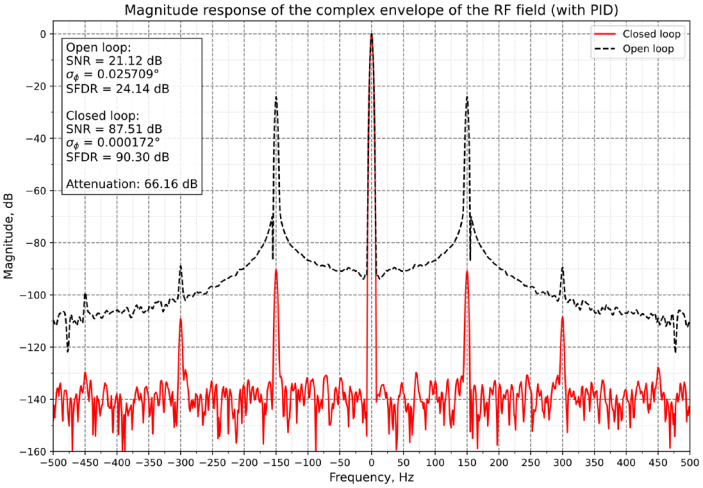

Fig. 7. Magnitude response of the complex envelope and results of field stability evaluation with a PID controller

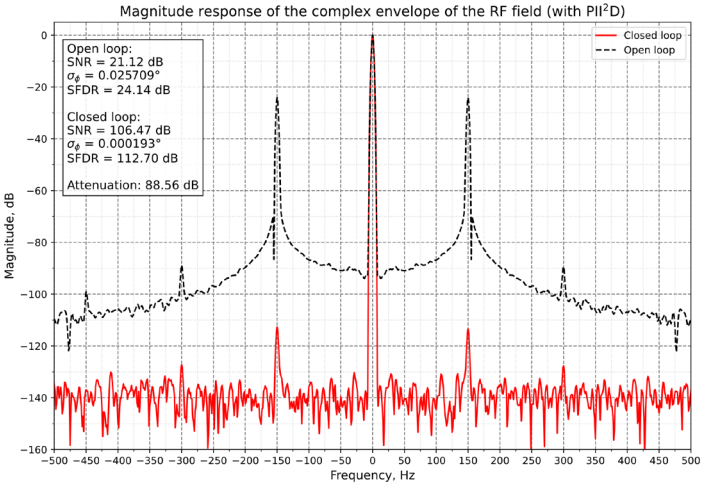

Fig. 8. Magnitude response of the complex envelope and results of field stability evaluation with a PII²D controller

The spurious-free dynamic range (SFDR) increases by more than 22 dB compared to the results obtained with the classical PID controller. In this experiment, phase fluctuations were not modeled, since stabilization is performed based on complex-envelope stabilization. It can be assumed that the RMS deviation of the initial phase σ_φ will also decrease by approximately an order of magnitude compared to a system with a classical PID controller.

9. Conclusion. This work considers the synthesis of a stabilization system for the parameters of the RF field in the resonant circuit of a charged-particle accelerator using a **PII²D**-type controller. A dynamic analysis of the system transfer functions has been performed, and the sensitivity frequency characteristics have been investigated. A hardware implementation of the **PII²D** controller has been carried out, and recommendations are provided for reducing the system settling time in LLRF systems of linear accelerators.

The main contribution of this work is the introduction of a controller structure with a second-order integral term that increases the system type and improves low-frequency disturbance rejection without requiring a priori knowledge of disturbance characteristics. In contrast to conventional PID-based approaches, the proposed method achieves a steeper sensitivity roll-off (-40 dB/decade) while preserving stability margins and maintaining implementation simplicity.

The simulation results show that the introduction of a second-order integral term significantly improves the suppression of low-frequency disturbances in the control loop. In this case, amplitude stability exceeding **106** dB is achieved, compared to typical values of modern stabilization systems on the order of **80-86** dB. At the same time, a significant reduction in the RMS deviation of the signal phase is observed—by at least an **order** of magnitude compared to modern systems.

However, such a control system may exhibit reduced robustness over a wider range of variations in the cavity quality factor during accelerator operation. In this case, the gain of the second-order integral component should be selected significantly lower in order to preserve the required stability margins and reduce the risk of oscillatory transients.

As a further development of this work, an experimental investigation of the proposed method in combination with feedforward control and adaptive feedforward control is planned. This will make it possible to evaluate the effectiveness of the combined approach in suppressing both low-frequency disturbances and repetitive pulse-to-pulse RF field errors in an LLRF system.

The obtained results confirm the effectiveness of using a controller with a second-order integral term for RF field stabilization tasks.

References

1. Simrock S.N. Achieving phase and amplitude stability in pulsed superconducting cavities. Proceedings of the Particle Accelerator Conference (PACS). IEEE. 2001. pp. 473–477. DOI: 10.1109/PAC.2001.987545.
2. Simrock S., et al. Low-Level Radio Frequency Systems. Cham: Springer, 2022. 382 p.
3. Liepe M., et al. A New Digital Control System for CESR-C and the Cornell ERL. Proceedings of the Particle Accelerator Conference. IEEE. 2003. pp. 3347–3349.
4. Shen Y.-B., et al. Impact of feedback loop parameter settings on the stability margin in a double radio-frequency system. Nuclear Science and Techniques. 2025. vol. 36. no. 109. pp. 1–14. DOI: 10.1007/s41365-025-01674-8.
5. Lee Y.-S., et al. Preliminary design study of prototype LLRF system for Korean-4GSR. Journal of the Korean Physical Society. 2023. vol. 83. pp. 640–646. DOI: 10.1007/s40042-023-00849-z.
6. Wang Q., et al. Low-level RF control system for BEPCII upgrade project. Radiation Detection Technology and Methods. 2026. DOI: 10.1007/s41605-026-00658-5.
7. Chen G., et al. Research and development of RF system for SC200 cyclotron. Journal of Physics: Conference Series. 2018. vol. 1067. 082003 p. DOI: 10.1088/1742-6596/1067/8/082003.
8. Lao C., et al. Fabrication and performance of the digital low-level RF control system for the 1.3 GHz buncher cavity. Proceedings of the International Conference on Microwave and Millimeter Wave Technology (ICMMT). IEEE. 2018. pp. 1–3.
9. Tu X., et al. The analysis of beam stability and improvement of RF system at HUST THz-FEL by digital LLRF. Nuclear Instruments and Methods in Physics Research Section A: Accelerators, Spectrometers, Detectors and Associated Equipment. 2021. vol. 1011. 165588 p. DOI: 10.1016/j.nima.2021.165588.

10. Schilcher T. RF applications in digital signal processing. CERN Accelerator School. 2008. pp. 249–257.
11. Duckitt W. A digital low-level radio frequency control system for the particle accelerators at iThemba LABS. Stellenbosch University. PhD dissertation. 2018.
12. Bortolato D., et al. New LLRF control system at LNL. Proceedings of the IEEE-NPSS Real Time Conference (RT). IEEE. 2016. pp. 1–8.
13. Tamura F., et al. Commissioning of the next-generation LLRF control system for the Rapid Cycling Synchrotron of the Japan Proton Accelerator Research Complex. Nuclear Instruments and Methods in Physics Research Section A: Accelerators, Spectrometers, Detectors and Associated Equipment. 2021. vol. 999. 165211 p. DOI: 10.1016/j.nima.2021.165211.
14. Fu X., et al. LLRF controller for high current cyclotron-based BNCT system. IEEE Transactions on Nuclear Science. 2021. vol. 68. no. 10. pp. 2452–2458.
15. Xiong Z., et al. The design of LLRF system for STCF storage ring. Modern Physics Letters A. 2024. vol. 39. no. 40. 2440001 p. DOI: 10.1142/S0217732324400017.
16. Wegmann C.J., et al. FAIR SIS100 accelerating RF system – Modeling and analysis of the coupled LLRF control loops. Journal of Physics: Conference Series. 2024. vol. 2687. 072034 p. DOI: 10.1088/1742-6596/2687/7/072034.
17. Zhang J., et al. A precision LLRF control system for UED. Nuclear Instruments and Methods in Physics Research Section A: Accelerators, Spectrometers, Detectors and Associated Equipment. 2021. vol. 1012. 165587 p.
18. Zenker K., et al. MicroTCA.4-based low-level RF for continuous wave mode operation at the ELBE accelerator.IEEE Transactions on Nuclear Science. 2021. vol. 68. no. 9. pp. 2326–2333. DOI: 10.1109/TNS.2021.3096757.
19. Chao C., et al. Design and performance of the digital LLRF control system for isotope production cyclotron. Journal of the Korean Physical Society. 2022. vol. 82. pp. 139–146. DOI: 10.1007/s40042-022-00641-5.
20. Li X., et al. CSNS-II multi-harmonic LLRF upgrade and commissioning. Journal of Instrumentation. 2024. vol. 19. T10006 p.
21. Li S., et al. Adaptive Feedforward Control Design Based on Simulink for J-PARC Linac LLRF System. Proceedings of the 9th International Particle Accelerator Conference (IPAC). JACoW Publishing. 2018. pp. 2187–2189. DOI: 10.18429/JACoW-IPAC2018-WEPAL017.
22. Vybornov A.S. PIID-controller-SystemVerilog. GitHub. Available at: https://github.com/happydispatch/PIID-controller-SystemVerilog-

Vybornov Aleksandr — Research intern, G. N. Flerov Laboratory of Nuclear Reactions (FLNR); author and supervisor, JINR Engineering and Science Workshop, Joint Institute for Nuclear Research (JINR); Postgraduate student, Department of Electronics Design for Megascience Facilities, Dubna State University. Research interests: digital signal processing, automatic control systems, FPGA. The number of publications — 3. vybornov.a.s@mail.ru; 6, Joliot-Curie St., 141980, Dubna, Russia; office phone: +7(496)216-4341.

Trofimov Aleksandr — Dr. Habil., Professor, Department “Design of Electronics for Mega-Science Facilities”, Dubna State University. Research interests: processing of data and digital signals, synthesis of automatic control systems, development of neural network technologies for information processing. The number of publications — 150. trofimov.a.t@uni-dubna.ru; 19, University St., 141980, Dubna, Russia; office phone: +7(496)216-6180.

Pashhenko Sergey — Head of Department, G. N. Flerov Laboratory of Nuclear Reactions (FLNR), Joint Institute for Nuclear Research (JINR). Research interests: development of

electronic equipment for accelerator complexes. The number of publications — 19. svpashch@jinr.ru; 6, Joliot-Curie St., 141980, Dubna, Russia; office phone: +7(496)216-4264.

Krylov Alexey — Lead engineer, G. N. Flerov Laboratory of Nuclear Reactions (FLNR), Joint Institute for Nuclear Research (JINR). Research interests: development of data acquisition and control devices, software for automatic control systems. The number of publications — 18. krylov@jinr.ru; 6, Joliot-Curie St., 141980, Dubna, Russia; office phone: +7(496)216-4405.

Shishkin Alexey — Senior engineer, G. N. Flerov Laboratory of Nuclear Reactions (FLNR), Joint Institute for Nuclear Research (JINR). Research interests: signal processing, automatic control systems, and electronic equipment development. The number of publications — 8. al64sh@mail.ru; 6, Joliot-Curie St., 141980, Dubna, Russia; office phone: +7(496)216-4341.

De-Monderik Olesya — Student, Faculty of Physical, Mathematical and Natural Sciences, Peoples' Friendship University of Russia named after Patrice Lumumba (RUDN). Research interests: digital signal processing, plasma physics, automatic control systems, spectral analysis. The number of publications — 1. 1032241330@rudn.ru; 3, Ordzhonikidze St., 115419, Moscow, Russia; office phone: +7(926)674-4106.

.

УДК 681.5:004.942 **DOI** 10.15622/ia.25.4.11

А.С. Выборнов, А.Т. Трофимов, С.В. Пащенко, А.И. Крылов,
А.А. Шишкин, О.Д. Де-Мондерик

ПОВЫШЕНИЕ СТАБИЛЬНОСТИ ВЧ ПОЛЯ В LLRF СИСТЕМЕ ЗА СЧЁТ ДОБАВЛЕНИЯ ИНТЕГРАЛЬНОЙ СОСТАВЛЯЮЩЕЙ ВТОРОГО ПОРЯДКА В ПЕРЕДАТОЧНУЮ ФУНКЦИЮ ПИД-РЕГУЛЯТОРА

Выборнов А.С., Трофимов А.Т., Пащенко С.В., Крылов А.И., Шишкин А.А., Де-Мондерик О.Д. **Повышение стабильности ВЧ поля в LLRF системе за счёт добавления интегральной составляющей второго порядка в передаточную функцию ПИД-регулятора.**

Аннотация. В работе рассматривается задача повышения точности стабилизации амплитуды и фазы высокочастотного поля в системе низкоуровневого радиочастотного управления (LLRF), применяемой в ускорителях заряженных частиц. Показано, что основным источником деградации стабильности являются низкочастотные возмущения, обусловленные пульсациями источников питания, температурными дрейфами и изменением параметров нагрузки. Продемонстрировано, что классическая структура ПИД-регулятора принципиально ограничена в подавлении таких возмущений вследствие компромисса между усилением на низких частотах и запасами устойчивости. Предложена модифицированная структура регулятора с интегральной составляющей второго порядка. Показано, что предложенный подход приводит к увеличению порядка астатизма системы и формированию наклона амплитудной характеристики -40 дБ/декаду в области низких частот, что обеспечивает существенно более эффективное подавление квазистационарных и медленно изменяющихся возмущений. Разработана математическая модель системы управления, отражающая основные динамические свойства ВЧ тракта. Дополнительно предложена нелинейная стратегия управления, основанная на отложенной активации интегральной составляющей второго порядка, которая предотвращает увеличение длительности переходного процесса при сохранении эффективности подавления возмущений. Результаты численного моделирования и экспериментальных исследований показывают, что предложенный регулятор обеспечивает увеличение динамического диапазона и стабильности амплитуды более чем на 20 дБ по сравнению с типичными современными системами, а также снижение среднеквадратичного отклонения фазы не менее чем на порядок. Полученные результаты подтверждают, что введение интегральной составляющей второго порядка в структуру регулятора является эффективным способом повышения точности стабилизации ВЧ сигнала при сохранении устойчивости и робастности системы управления.

Ключевые слова: стабилизация ВЧ поля, LLRF система, ВЧ тракт, ПЛИС, подавление низкочастотных искажений, ВЧ система циклотрона.

Литература

1. Simrock S.N. Achieving phase and amplitude stability in pulsed superconducting cavities // Proceedings of the Particle Accelerator Conference (PACS). IEEE. 2001. pp. 473–477. DOI: 10.1109/PAC.2001.987545.
2. Simrock S., et al. Low-Level Radio Frequency Systems // Cham: Springer, 2022. 382 p.
3. Liepe M., et al. A New Digital Control System for CESR-C and the Cornell ERL // Proceedings of the Particle Accelerator Conference. IEEE. 2003. pp. 3347–3349.

4. Shen Y.-B., et al. Impact of feedback loop parameter settings on the stability margin in a double radio-frequency system // Nuclear Science and Techniques. 2025. vol. 36. no. 109. pp. 1–14. DOI: 10.1007/s41365-025-01674-8.
5. Lee Y.-S., et al. Preliminary design study of prototype LLRF system for Korean-4GSR // Journal of the Korean Physical Society. 2023. vol. 83. pp. 640–646. DOI: 10.1007/s40042-023-00849-z.
6. Wang Q., et al. Low-level RF control system for BEPCII upgrade project // Radiation Detection Technology and Methods. 2026. DOI: 10.1007/s41605-026-00658-5.
7. Chen G., et al. Research and development of RF system for SC200 cyclotron // Journal of Physics: Conference Series. 2018. vol. 1067. 082003 p. DOI: 10.1088/1742-6596/1067/8/082003.
8. Lao C., et al. Fabrication and performance of the digital low-level RF control system for the 1.3 GHz buncher cavity // Proceedings of the International Conference on Microwave and Millimeter Wave Technology (ICMMT). IEEE. 2018. pp. 1–3.
9. Tu X., et al. The analysis of beam stability and improvement of RF system at HUST THz-FEL by digital LLRF // Nuclear Instruments and Methods in Physics Research Section A: Accelerators, Spectrometers, Detectors and Associated Equipment. 2021. vol. 1011. 165588 p. DOI: 10.1016/j.nima.2021.165588.
10. Schilcher T. RF applications in digital signal processing // CERN Accelerator School. 2008. pp. 249–257.
11. Duckitt W. A digital low-level radio frequency control system for the particle accelerators at iThemba LABS // Stellenbosch University. PhD dissertation. 2018.
12. Bortolato D., et al. New LLRF control system at LNL. Proceedings of the IEEE-NPSS Real Time Conference (RT). IEEE. 2016. pp. 1–8.
13. Tamura F., et al. Commissioning of the next-generation LLRF control system for the Rapid Cycling Synchrotron of the Japan Proton Accelerator Research Complex // Nuclear Instruments and Methods in Physics Research Section A: Accelerators, Spectrometers, Detectors and Associated Equipment. 2021. vol. 999. 165211 p. DOI: 10.1016/j.nima.2021.165211.
14. Fu X., et al. LLRF controller for high current cyclotron-based BNCT system // IEEE Transactions on Nuclear Science. 2021. vol. 68. no. 10. pp. 2452–2458.
15. Xiong Z., et al. The design of LLRF system for STCF storage ring. Modern Physics Letters A. 2024. vol. 39. no. 40. 2440001 p. DOI: 10.1142/S0217732324400017.
16. Wegmann C.J., et al. FAIR SIS100 accelerating RF system – Modeling and analysis of the coupled LLRF control loops // Journal of Physics: Conference Series. 2024. vol. 2687. 072034 p. DOI: 10.1088/1742-6596/2687/7/072034.
17. Zhang J., et al. A precision LLRF control system for UED // Nuclear Instruments and Methods in Physics Research Section A: Accelerators, Spectrometers, Detectors and Associated Equipment. 2021. vol. 1012. 165587 p.
18. Zenker K., et al. MicroTCA.4-based low-level RF for continuous wave mode operation at the ELBE accelerator // IEEE Transactions on Nuclear Science. 2021. vol. 68. no. 9. pp. 2326–2333. DOI: 10.1109/TNS.2021.3096757.
19. Chao C., et al. Design and performance of the digital LLRF control system for isotope production cyclotron // Journal of the Korean Physical Society. 2022. vol. 82. pp. 139–146. DOI: 10.1007/s40042-022-00641-5.
20. Li X., et al. CSNS-II multi-harmonic LLRF upgrade and commissioning // Journal of Instrumentation. 2024. vol. 19. T10006 p.
21. Li S., et al. Adaptive Feedforward Control Design Based on Simulink for J-PARC Linac LLRF System // Proceedings of the 9th International Particle Accelerator Conference (IPAC). JACoW Publishing. 2018. pp. 2187–2189. DOI: 10.18429/JACoW-IPAC2018-WEPAL017.

22. Vybornov A.S. PIID-controller-SystemVerilog // GitHub. URL: https://github.com/happydispatch/PIID-controller-SystemVerilog-

Выборнов Александр Сергеевич — стажёр-исследователь, лаборатория ядерных реакций имени Г. Н. Флёрова (ЛЯР); автор и руководитель, инженерно-научный практикум УНЦ ОИЯИ, Объединённый институт ядерных исследований (ОИЯИ); аспирант, кафедра «проектирование электроники для установок «мегасайенс», Федеральное государственное бюджетное образовательное учреждение высшего образования «Университет „Дубна“». Область научных интересов: цифровая обработка сигналов, системы автоматического управления, ПЛИС. Число научных публикаций — 3. vybornov.a.s@mail.ru; улица Жолио-Кюри, 6, 141980, Дубна, Россия; р.т.: +7(496)216-4341.

Трофимов Александр Терентьевич — д-р техн. наук, профессор, профессор, кафедра «проектирование электроники для установок «мегасайенс», Федеральное государственное бюджетное образовательное учреждение высшего образования «Университет „Дубна“». Область научных интересов: работка данных и цифровых сигналов, синтез систем автоматического управления, разработка нейросетевых технологий обработки информации. Число научных публикаций — 150. trofimov.a.t@uni-dubna.ru; Университетская улица, 19, 141980, Дубна, Россия; р.т.: +7(496)216-6180.

Пащенко Сергей Васильевич — начальник отдела, лаборатория ядерных реакций имени Г. Н. Флёрова (ЛЯР), Объединённый институт ядерных исследований (ОИЯИ). Область научных интересов: разработка электронной аппаратуры для ускорительных комплексов. Число научных публикаций — 19. svpashch@jinr.ru; улица Жолио-Кюри, 6, 141980, Дубна, Россия; р.т.: +7(496)216-4264.

Крылов Алексей Иванович — ведущий инженер, лаборатория ядерных реакций имени Г. Н. Флёрова (ЛЯР), Объединённый институт ядерных исследований (ОИЯИ). Область научных интересов: разработка устройств сбора данных и управления, программное обеспечение для систем автоматического управления. Число научных публикаций — 18. krylov@jinr.ru; улица Жолио-Кюри, 6, 141980, Дубна, Россия; р.т.: +7(496)216-4405.

Шишкин Алексей Александрович — старший инженер, лаборатория ядерных реакций имени Г. Н. Флёрова (ЛЯР), Объединённый институт ядерных исследований (ОИЯИ). Область научных интересов: обработка сигналов, системы автоматического управления, разработка электронной аппаратуры. Число научных публикаций — 8. al64sh@mail.ru; улица Жолио-Кюри, 6, 141980, Дубна, Россия; р.т.: +7(496)216-4341.

Де-Мондерик Олеся Дмитриевна — студент, факультет физико-математических и естественных наук, Федеральное государственное автономное образовательное учреждение высшего образования "Российский университет дружбы народов имени Патриса Лумумбы" (РУДН). Область научных интересов: цифровая обработка сигналов, физика плазмы, системы автоматического управления, спектральный анализ. Число научных публикаций — 1. 1032241330@rudn.ru; улица Орджоникидзе, 3, 115419, Москва, Россия; р.т.: +7(926)674-4106.